Energy Landscapes and the Non-Newtonian Viscosity of Liquids and Glasses

Daniel J. Lacks

Department of Chemical Engineering, Tulane University, New Orleans, Louisiana 70118

(Received 4 December 2000; published 13 November 2001)

An inherent structure analysis of viscosity is developed based on results of nonequilibrium molecular dynamics simulations. The viscosity is separated into a "structural" contribution associated with the energy minima that the system visits, and a "vibrational" contribution associated with displacements within the energy minima. The structural contribution is shear thinning due to strain-activated relaxations caused by the disappearance of high-stress energy minima, while the vibrational contribution is Newtonian.

DOI: 10.1103/PhysRevLett.87.225502 PACS numbers: 61.43.Fs, 47.50.+d, 61.20.Lc, 66.20.+d

The viscosity of liquids, both molecular and colloidal, generally decreases with increasing shear rate at high shear rates. This "shear thinning" occurs even for systems composed of spherical particles, as found in experiments on colloidal systems [1] and simulations of simple molecular systems [2]. The present investigation addresses the origins of shear thinning in terms of the potential energy landscape, using the inherent structure formalism of Stillinger and Weber [3].

The inherent structure formalism separates the dynamics of liquids into vibrational motion within local potential energy minima ("inherent structures"), and structural transitions between different local minima [3]. Material properties can then be considered as the sum of "structural" contributions that are evaluated at the local energy minima that the system visits, and "vibrational" contributions that are associated with atomic displacements within these local minima (the local minima that the system visits are defined as those obtained by steepest-descent quenches from instantaneous atomic configurations during a molecular dynamics trajectory [4]). This formalism does not introduce any approximations, but rather is a method of dividing effects in a physically meaningful way.

Nonequilibrium molecular dynamics (NEMD) simulations are carried out on a flowing liquid at shear rate γ. The sllod equations of motion are used with Lees-Edwards boundary conditions and a Gaussian thermostat [5,6]. The system examined is a binary (80%–20%) mixture of Lennard-Jones atoms that prevents crystallization [7]. The Lennard-Jones parameters are ε_{ij} and σ_{ij} for interactions between atoms of type i and type j, where $\varepsilon_{22} = 0.5\varepsilon_{11}$, $\sigma_{22} = 0.88\sigma_{11}$, $\varepsilon_{12} = 1.5\varepsilon_{11}$, and $\sigma_{12} = 0.8\sigma_{11}$; the interactions are truncated at the distance of $2.5\sigma_{ij}$ (and shifted such that the energy is continuous at the truncation distance). All of the atoms have the same mass m. The units used throughout the paper are ε_{11} for energy, σ_{11} for length, ε_{11}/k_B for temperature, $(m{\sigma_{11}}^2/\varepsilon_{11})^{1/2}$ for time, $\varepsilon_{11}/{\sigma_{11}}^3$ for stress, and $(m\varepsilon_{11}/{\sigma_{11}}^4)^{1/2}$ for viscosity. The simulations are carried out for $N = 500$ atoms at the density $\rho = 1.2$, for 10^6–10^7 NEMD steps (depending on the shear rate) with a time step of 0.01. The shear stress τ is calculated during the NEMD trajectory [5], and the viscosity μ is obtained as $\mu = \langle\tau\rangle/\gamma$, where $\langle\cdots\rangle$ represents an average over the NEMD trajectory.

The results for the viscosity as a function of shear rate are shown in Fig. 1. The present results are in good agreement with previous results for the same system [8]. The viscosity is nearly Newtonian (i.e., constant) for all shear rates examined at the temperature $T = 0.7$, while the viscosity is strongly shear thinning (i.e., decreasing with increasing shear rate) for all shear rates examined at $T = 0.3$. At $T = 0.5$, the viscosity is slightly shear thinning at smaller shear rates, and strongly shear thinning at higher shear rates. As found previously [8], these driven systems reach reproducible steady states even at temperatures below the glass transition temperature [this effect is demonstrated in Fig. 5b (below), which shows that the same results are obtained from different starting points].

Energy minima that the system visits are found by carrying out energy minimizations that begin from instantaneous configurations during the NEMD trajectory (these minimizations do not affect the NEMD trajectory); the energy minima are found at time intervals of 10–100 (depending on the shear rate). The energy (e) and shear stress are evaluated at these energy minima, and averaged to give $\langle e\rangle_s$ and $\langle\tau\rangle_s$, where $\langle\cdots\rangle_s$ represents an average over the ensemble of energy minima visited during the NEMD

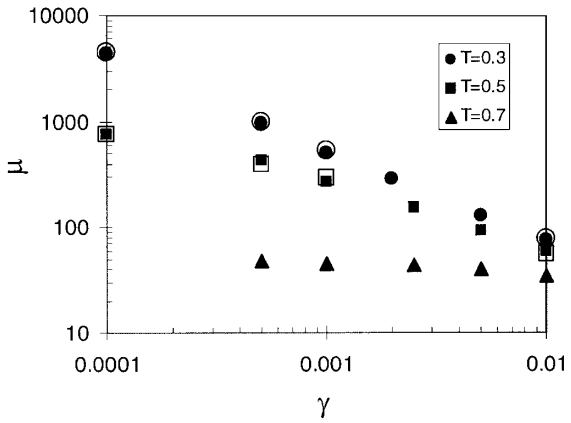

FIG. 1. Viscosity as a function of shear rate. Filled symbols are the present results, and open symbols are results from Ref. [8].

trajectory. The vibrational contribution to the average shear stress is determined as $\langle\tau\rangle_v = \langle\tau\rangle - \langle\tau\rangle_s$.

The structural and vibrational contributions to the shear stress are shown in Fig. 2. The value of $\langle\tau\rangle_v$ increases linearly with increasing shear rate for all shear rates; noting that $\mu = \langle\tau\rangle/\gamma$, the vibrational contribution is seen to be Newtonian for all shear rates examined. In contrast, the value of $\langle\tau\rangle_s$ increases with increasing shear rate at low shear rates, but then levels off and does not exceed an upperbound [9]; again noting that $\mu = \langle\tau\rangle/\gamma$, the structural contribution is seen to be shear thinning. The shear thinning of the overall viscosity is therefore attributable solely to the structural contribution.

To understand why the structural contribution to the shear stress is shear thinning, zero-temperature time-independent simulations are run in which the shear strain is incremented in very small steps, with energy minimizations carried out after each step (these simulations start from instantaneous configurations during the NEMD trajectory). As shown in Fig. 3 for a single configuration, the shear stress and energy at an energy minimum usually increase continuously with strain, but these increases are punctuated by discontinuous drops; analogous results have also been found in similar simulations on other systems [10–13]. Our previous investigations have shown that these discontinuous stress and energy drops occur when strain causes a local energy minimum to flatten until it disappears [14–16], as shown schematically in Fig. 4. Thus the shear stress *at energy minima* (i.e., the structural contribution) cannot increase indefinitely with strain, because energy minima characterized by high stress do not exist.

If strain causes the disappearance of the energy minimum that the system is in, the system is forced towards an alternate (lower-stress) energy minimum—these transitions to alternate energy minima are strain-activated relaxations, which can become important at high strain rates.

The temperature dependence of $\langle\tau\rangle_s$, shown in Fig. 2, can be understood in that higher temperatures increasingly cause the system to exit an energy minimum by a thermally activated process before the minimum disappears. In this way, higher temperatures cause $\langle\tau\rangle_s$ to reach its upperbound at higher shear rates, and cause this upperbound to decrease in magnitude. As shown in Fig. 2b, the NEMD results for the upperbound of $\langle\tau\rangle_s$ extrapolate in the limit of low temperature towards the zero-temperature result in which the magnitude of the shear stress is limited solely by the disappearance of energy minima.

Recent work has shown that, at different temperatures, a liquid visits different regions of the energy landscape, characterized by different values of the average energy of the local minima visited, $\langle e\rangle_s$ [17]. The unique correspondence between T and $\langle e\rangle_s$ in equilibrium systems defines an effective temperature T_{eff} that increases monotonically with increasing $\langle e\rangle_s$ [18]. Our results for $\langle e\rangle_s$ as a function of shear rate and temperature are shown in Fig. 5. The value of $\langle e\rangle_s$ increases with increasing shear rate, in agreement with previous ideas [8]. At constant shear rate, $\langle e\rangle_s$ increases with increasing T for $T \gtrsim 0.45$, but

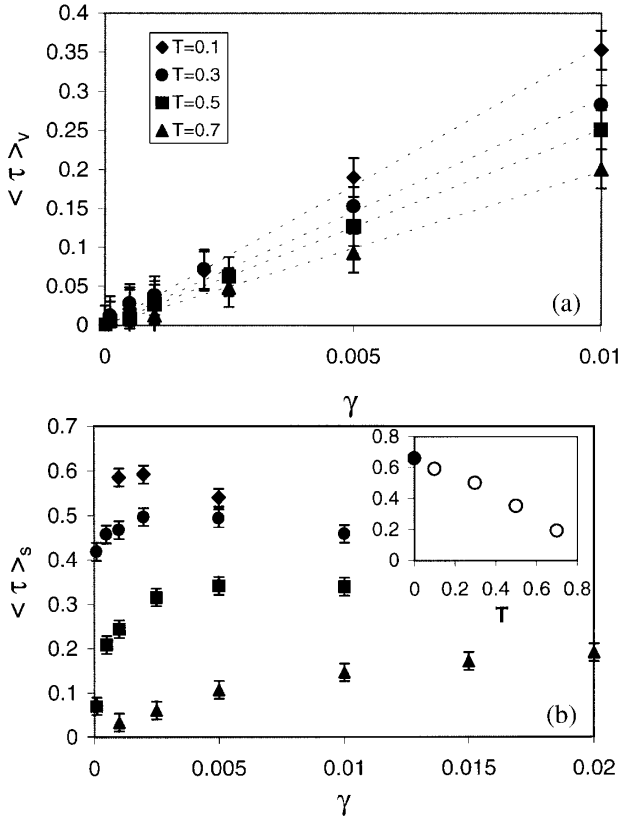

FIG. 2. (a) Vibrational contribution and (b) structural contribution to shear stress as a function of shear rate. Inset to (b) shows the upperbound of the structural contribution to the average shear stress, as a function of temperature [in the inset, open symbols are NEMD results, and the closed symbol is average shear stress in the zero-temperature (time-independent) simulations].

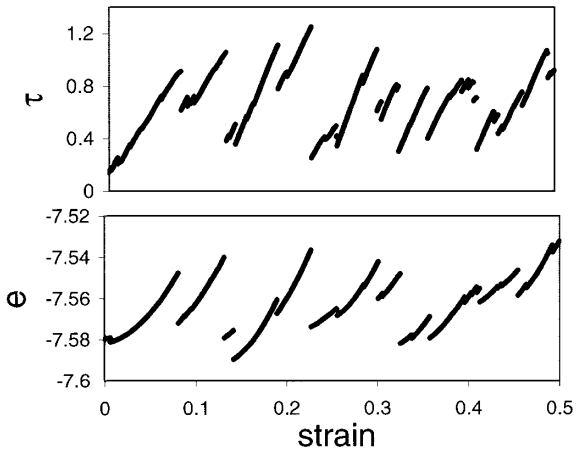

FIG. 3. Shear stress and energy (per atom) as a function of shear strain, for a single configuration that remains at a local energy minimum. The strain is incremented in steps of 0.0001, with energy minimizations carried out after each step. These results are time independent and at zero temperature.

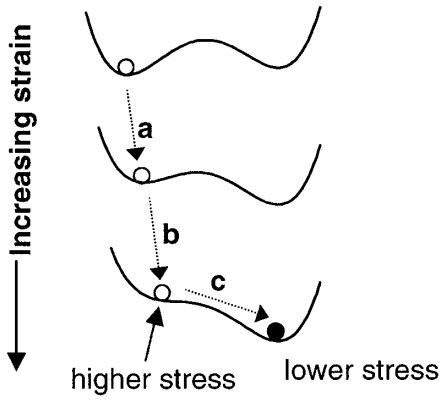

FIG. 4. Schematic of a strain-induced disappearance of an energy minimum. The curves represent the potential energy along the relevant coordinate, and the circles represent the state of the system. The change in the state of the system denoted by arrow "c" corresponds to a strain-activated relaxation process.

decreases with increasing T for $T \lesssim 0.45$. These results can be understood as follows: For $T \lesssim 0.45$, increased T enables the system to increasingly surmount energy barriers and reach lower energy regions of the landscape (which partially offsets the shear-induced increase in energy). For $T \gtrsim 0.45$, increased T moves the system to higher energy regions of the landscape (as in undriven systems [17,18]). Note that this change in behavior occurs very close to the mode coupling crossover temperature for this system ($T = 0.435$) [7]. Also shown in Fig. 5b is the result for $\langle e \rangle_s$ from the zero-temperature time-independent simulations, which correspond to NEMD simulations in the limits $T \to 0$ and $\gamma \to 0$; the NEMD results extrapolate to the zero-temperature time-independent result in these limits.

Neither the viscosity nor the structural contribution to the viscosity ($\langle \tau \rangle_s / \gamma$) are uniquely determined by $\langle e \rangle_s$ (or equivalently T_{eff}), and these quantities do not always follow the same trends as $\langle e \rangle_s$ (results shown in Fig. 5 for $\langle \tau \rangle_s / \gamma$; results not shown for μ). Note that the regions of the energy landscape visited at higher shear rates differ from those visited at higher temperatures (and $\gamma = 0$), in that the energy minima visited at higher shear rates are characterized by nonzero average shear stress (see Fig. 2), while the energy minima visited at higher temperatures (and $\gamma = 0$) are characterized by zero average shear stress.

The present results can be related to previous results for shear-rate dependence of the incoherent scattering function of supercooled liquids [8,19], by noting that the fast decay of the incoherent scattering function arises from vibrational contributions to the dynamics, while the slow decay arises from structural contributions [20]. The previous result that the fast decay is shear-rate independent [8,19] coincides with the present result that the vibrational contribution to the viscosity is shear-rate independent (Newtonian). Also, the previous result that the time scale of the slow decay decreases almost proportionally to the shear rate at low temperature [8,19] can be understood in that the dominant relaxation processes at low temperature (and high shear rates) are strain-activated processes, which have rates that are proportional to the shear rate.

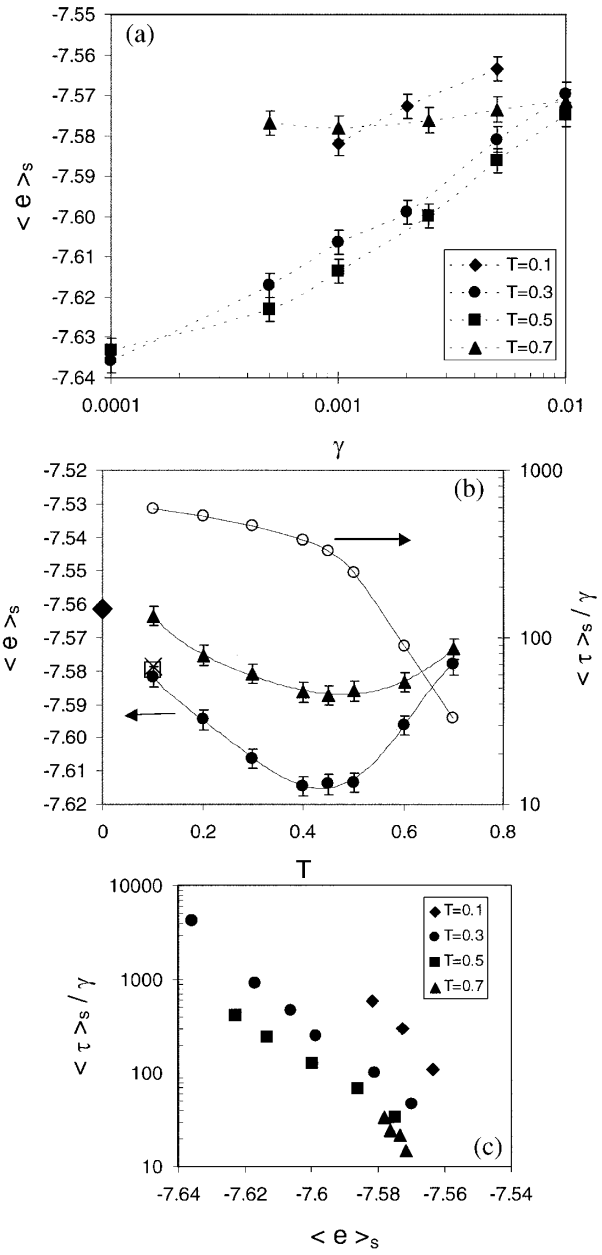

FIG. 5. (a) Average energy (per atom) of local minima visited as a function of shear rate; the lines are guides to the eye. Note that $\langle e \rangle_s$ has a unique and reproducible steady-state value at all temperatures in these driven systems, in contrast to undriven systems [18]. (b) Average energy of local minima visited and the structural contribution to the viscosity as a function of temperature. Circles: $\gamma = 0.001$; triangles: $\gamma = 0.005$; diamond: average energy in zero-temperature (time-independent) simulations. Also shown are results for $\langle e \rangle_s$ at $T = 0.1$, $\gamma = 0.001$ obtained from simulations beginning from the final configurations of the runs at $T = 0.5$, $\gamma = 0.001$ (cross) and $T = 0.1$, $\gamma = 0.005$ (square); the similarity of the results from the different starting conditions demonstrates that $\langle e \rangle_s$ has a unique and reproducible steady-state value. (c) Structural contribution to the viscosity as a function of the average energy of local minima visited.

The shear stress of strongly supercooled liquids is dominated by the structural contribution, which is nearly independent of shear rate (e.g., see results in Fig. 2 for low temperatures). Since the viscosity $\mu = \langle\tau\rangle/\gamma$, the viscosity of such strongly supercooled liquids will vary as $\mu \sim \gamma^{-1}$. This result concurs with experimental results for strongly supercooled liquids that show that $\mu \sim \gamma^{-1}$ [21,22].

The rate of strain-activated relaxations is proportional to the strain rate, and at high strain rates it can become comparable to the rate of thermally activated relaxations in a typical liquid. Under such high strain rates, the viscosity becomes comparable to the viscosity of a typical liquid, even if the undriven system behaves similar to a glass. Such a result has been found in nanoshock experiments [23], which show that $\mu \approx 3$ GPa s for glassy polymethylmethacrylate at a strain rate of $\sim 10^{10}$ s^{-1} (although the flow in these nanoshock experiments is not shear flow, the ideas developed here are expected to apply for all types of flows).

The picture that emerges from this inherent structure analysis is similar to the Eyring model for viscosity [24]; the present analysis differs in that it is not phenomenological, but based on NEMD results and mappings of the potential energy landscape for a real system. The main points of this picture, particularly the strain-induced disappearance of energy minima that lead to strain-activated relaxation processes, arise independently of the NEMD methodology—evidence for this is that the NEMD results extrapolate in the limit of low T to $T = 0$ results obtained by a different (time-independent) methodology (Figs. 2b and 5b).

An equivalent description of this physical picture is that shear flow causes the system to occupy different regions of the energy landscape, which are characterized by local minima with both higher energy (Fig. 5b) and higher shear stress (Fig. 2b). The system moves to these other regions of the landscape by remaining in a local minimum while shear strain distorts the local minimum such that its energy and shear stress increase (Fig. 3); this mechanism will become operative when the shear rate becomes comparable to the rate of structural transitions between energy minima. These higher-stress regions have lower energy barriers *for structural transitions that reduce the stress* (these energy barriers decrease to zero as the stress becomes high, as indicated by the discontinuous stress drops in Fig. 3)—these lower barriers lead to increased relaxation rates, which in turn decrease the viscosity (shear thinning).

Funding for this project was provided by the NSF (Grants No. DMR-9624808 and No. DMR-0080191).

[1] W. B. Russel, D. A. Saville, and W. R. Schowalter, *Colloidal Dispersions* (Cambridge University Press, Cambridge, England, 1989).
[2] D. J. Evans, Phys. Rev. A **23**, 1988 (1981).
[3] F. H. Stillinger and T. A. Weber, Science **225**, 983 (1984); F. H. Stillinger, Science **267**, 1935 (1995).
[4] F. H. Stillinger, P. G. Debenedetti, and S. Sastry, J. Chem. Phys. **109**, 3983 (1998).
[5] D. J. Evans and G. P. Morriss, *Statistical Mechanics of Nonequilibrium Liquids* (Academic, London, 1990).
[6] D. J. Evans, G. P. Morris, and L. M. Hood, Mol. Phys. **68**, 637 (1989).
[7] W. Kob and H. C. Anderson, Phys. Rev. Lett. **73**, 1376 (1994).
[8] J.-L. Barrat and L. Berthier, Phys. Rev. E **63**, 012503 (2001).
[9] At extremely high shear rates, the structural contribution to the shear stress decreases with shear rate, as shown in Fig. 2a. The physical significance of this result is questionable, and this result may be an artifact of the thermostating procedure, which becomes unphysical at very high shear rates.
[10] D. Deng, A. S. Argon, and S. Yip, Philos. Trans. R. Soc. London A **329**, 613 (1989).
[11] P. H. Mott, A. S. Argon, and U. W. Suter, Philos. Mag. A **67**, 931 (1993).
[12] C. F. Fan, Macromolecules **28**, 5215 (1995).
[13] M. Utz, P. G. Debenedetti, and F. H. Stillinger, Phys. Rev. Lett. **84**, 1471 (2000).
[14] D. L. Malandro and D. J. Lacks, Phys. Rev. Lett. **81**, 5576 (1998).
[15] D. J. Lacks, Phys. Rev. Lett. **80**, 5385 (1998).
[16] D. L. Malandro and D. J. Lacks, J. Chem. Phys. **110**, 4593 (1999).
[17] S. Sastry, P. G. Debenedetti, and F. H. Stillinger, Nature (London) **393**, 554 (1998).
[18] W. Kob, F. Sciortino, and P. Tartaglia, Europhys. Lett. **49**, 590 (2000).
[19] R. Yamamoto and A. Onuki, Phys. Rev. E **58**, 3515 (1998).
[20] T. B. Schroder, S. Sastry, J. C. Dyre, and S. C. Glotzer, J. Chem. Phys. **112**, 9834 (2000).
[21] J. H. Simmons, R. K. Mohr, and C. J. Montrose, J. Appl. Phys. **53**, 4075 (1982).
[22] R. L. Sammler *et al.,* J. Rheol. **40**, 285 (1996).
[23] H. Kim, S. A. Hambir, and D. D. Dlott, J. Phys. Chem. B **104**, 4239 (2000).
[24] H. Eyring, J. Chem. Phys. **4**, 283 (1936).